JOURNAL OF CELLULAR PHYSIOLOGY 207:767–774 (2006)

Subcutaneous Tissue Fibroblast Cytoskeletal Remodeling Induced by Acupuncture: Evidence for a Mechanotransduction-Based Mechanism

HELENE M. LANGEVIN,[1]* NICOLE A. BOUFFARD,[1] GARY J. BADGER,[2]
DAVID L. CHURCHILL,[1] AND ALAN K. HOWE[3]

[1]*Department of Neurology,* [2]*Department of Medical Biostatistics,*
[3]*Department of Pharmacology, Vermont Cancer Center,*
University of Vermont College of Medicine, Burlington Vermont

Acupuncture needle rotation has been previously shown to cause specific mechanical stimulation of subcutaneous connective tissue. This study uses acupuncture to investigate the role of mechanotransduction-based mechanisms in mechanically-induced cytoskeletal remodeling. The effect of acupuncture needle rotation was quantified by morphometric analysis of mouse tissue explants imaged with confocal microscopy. Needle rotation induced extensive fibroblast spreading and lamellipodia formation within 30 min, measurable as an increased in cell body cross sectional area. The effect of rotation peaked with two needle revolutions and decreased with further increases in rotation. Significant effects of rotation were present throughout the tissue, indicating the presence of a response extending laterally over several centimeters. The effect of rotation with two needle revolutions was prevented by pharmacological inhibitors of actomyosin contractility (blebbistatin), Rho kinase (Y-27632 and H-1152), and Rac signaling. The active cytoskeletal response of fibroblasts demonstrated in this study constitutes an important step in understanding cellular mechanotransduction responses to externally applied mechanical stimuli in whole tissue, and supports a previously proposed model for the mechanism of acupuncture involving connective tissue mechanotransduction. J. Cell. Physiol. 207: 767–774, 2006. © 2006 Wiley-Liss, Inc.

Subcutaneous tissue is part of a network of "loose" connective tissue extending throughout the body including fasciae and interstitial connective tissue. This web of tissue is populated by an interconnected network of fibroblasts that rapidly respond to tissue stretch (within minutes) with active, dynamic, and reversible changes in cell shape (Langevin et al., 2004, 2005). Unlike dermis and load bearing connective tissues (e.g., ligament, tendon), subcutaneous tissue has a low tensile modulus close to that of cells (Iatridis et al., 2003). Thus fibroblasts within loose connective tissues may perceive a greater range of externally applied forces than those embedded in a denser collagen matrix. These recent findings suggest that loose connective tissue may actively and rapidly respond to changing tissue loads. Understanding the cellular mechanisms underlying these responses is central to establishing the nature of this new and potentially important physiological function.

The cytoskeleton has emerged as a key structural element allowing transmission of externally applied mechanical forces to the cell and conversion of these forces into biochemical responses (Chicurel et al., 1998, 2003). Indeed, the cytoskeleton's plasticity, mechanical responsiveness, and links to key intracellular regulatory proteins such as Rho GTPases form the basis of mechanotransduction (Banes et al., 1995; Hall, 1998). Because mechanotransduction concerns interactions of the cell with its environment, studying mechanotransduction mechanisms in whole tissues is an important complement to cell culture models. This is especially important for connective tissue, since its extracellular matrix and mechanical environment are much more complex than even "3-d" cell culture conditions (Grinnell, 2003). In this context, the ancient technique of acupuncture provides a useful experimental tool to investigate mechanotransduction within connective tissue. It was recently shown that, during acupuncture, rotation of the acupuncture needle causes winding of subcutaneous tissue (but not dermis), and pulling of the loose collagen bundles from the periphery toward the needle (Langevin et al., 2001a). In rats, needle rotation produced measurable changes in subcutaneous tissue matrix architecture together with a tenfold increase in the amount of force necessary to pull the needle out of the tissue (Langevin et al., 2002). A unique feature of acupuncture therefore is that, unlike stretching of whole skin, needle rotation specifically probes the loose subcutaneous tissue layer. Thus, acupuncture allows investigation of cellular responses to a highly-specific mechanical stimulus.

In this study, we have used acupuncture to investigate the role of mechanotransduction-based signaling mechanisms in mechanically-induced cytoskeletal

Contract grant sponsor: National Center for Complementary and Alternative Medicine (NCCAM); Contract grant number: RO1 AT01121.

*Correspondence to: Dr. Helene M. Langevin, Department of Neurology, University of Vermont College of Medicine, Given C423, 89 Beaumont Avenue, Burlington, VT 05405.
E-mail: helene.langevin@uvm.edu

Received 7 November 2005; Accepted 10 January 2006

DOI: 10.1002/jcp.20623

remodeling. We hypothesized that, in mouse whole skin tissue explants, acupuncture needle rotation induces dose-dependent morphological changes in subcutaneous tissue fibroblasts, and that these changes involve Rho and Rac signaling mechanisms as well as actomyosin contractility. In addition to investigating basic cellular physiological processes, this approach may eventually contribute to a better understanding of how connective tissue mechanotransduction may be part of acupuncture's therapeutic mechanism.

MATERIALS AND METHODS

Experiment setup and protocol

Experimental protocols were approved by the University of Vermont IACUC. C57Black-6 mice (19–24 g) were sacrificed by decapitation. Immediately after death, an 8 cm by 3 cm tissue flap containing dermis, subcutaneous muscle, and subcutaneous tissue was excised from the back of each mouse. Excision involved minimal cutting of the loose cleavage plane separating the subcutaneous tissue layer from the back muscles. Tissue flaps were placed transversely in grips and immersed in an incubation bath containing 37°C HEPES-physiological saline pH 7.4 as previously described and placed vertically in a holder with the proximal grip connected to a 500*g* (4.9 N) capacity load cell (Langevin et al., 2005). The tissue was elongated at a rate of 1 mm/sec by advancing a micrometer connected to the distal tissue grip until a varying amount of preload was achieved. The tissue length was then fixed by attaching a pair of stabilization bars. Tissue and grips together were then disconnected from the load cell and placed under a dissecting microscope. An acupuncture needle (Seirin, Japan, 0.25 mm diameter, and 50 mm length) was inserted parallel to the dermis, carefully "tunneling" the needle through the middle of the subcutaneous tissue layer (Fig. 1A). Extreme care was taken during this procedure to insert the needle without pulling on the tissue. The tissue and grips were then placed back into the incubation bath. A modified version of a computer-controlled acupuncture needling instrument (Langevin et al., 2001b) was used to perform needle rotation (Fig. 1). The instrument's motor was attached to the needle and placed into a clamp to maintain the needle in a fixed vertical position during rotation (Fig. 1B). The needle was rotated immediately (to mimic the clinical situation in which needles are usually manipulated directly following insertion) with a varying number of clockwise needle revolutions (or not rotated) at a constant speed (1 rev/sec) and acceleration of 3 revs/sec^2. After needle rotation, the motor was disconnected and the tissue was further incubated for 30 min. The tissue was then immersion fixed in 95% ethanol for 1 h, then rinsed overnight in phosphate-buffered saline (PBS) /1.0% Bovine serum albumin at 4°C with the needle in place.

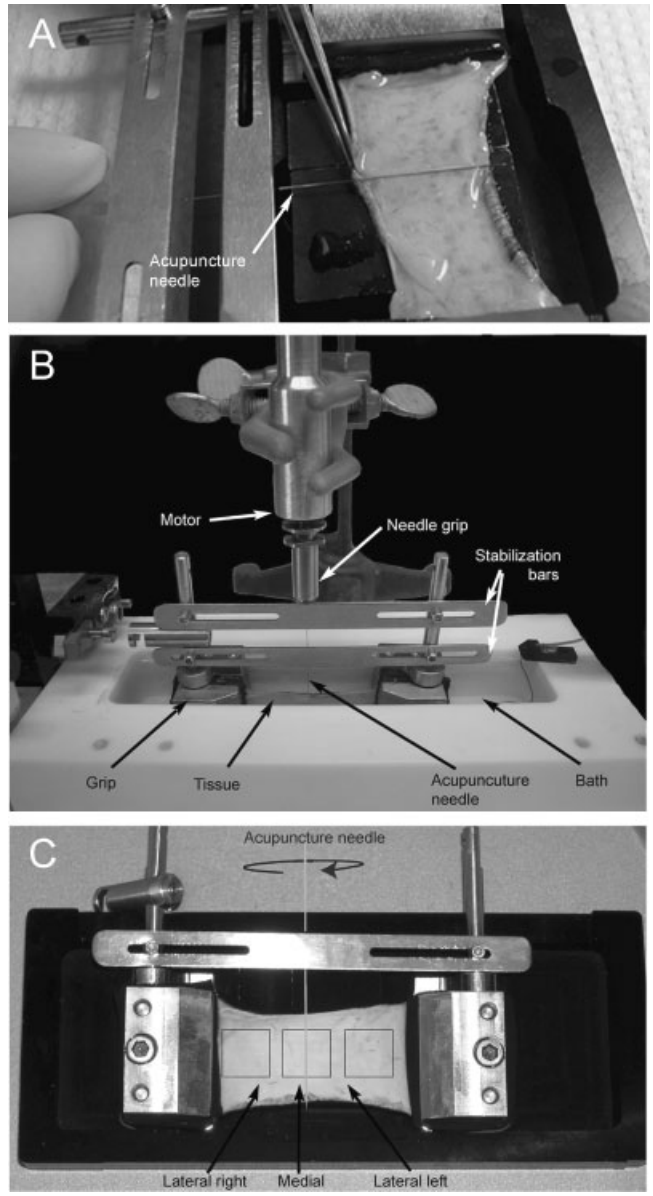

Fig. 1. Experimental setup. **A**: Excised mouse tissue after preload and during the acupuncture needle insertion procedure. **B**: Excised mouse tissue is maintained at 37°C at a fixed length after setting tissue preload. An acupuncture needle inserted into the subcutaneous tissue is attached to a needle grip and motor (needle grips placed vertically in bath). **C**: Location of subcutaneous tissue samples relative to the needle (needle parallel to skin).

Experimental design and variables

Varying preload with no rotation. To establish the optimal tissue preload for needle rotation experiments (defined as the maximum amount of preload that would not by itself cause detectable cellular changes), tissue flaps were elongated until a load of, 1.96 mN (equivalent to a 0.2 g mass), 2.9 mN (0.3 g), or 4.9 mN (0.5 g) was achieved.

Constant preload with varying rotation. Tissue flaps were elongated to a preload of 2.9 mN followed by either, 0, 2, 4, 8, or 12 clockwise needle revolutions.

Pharmacological experiments with two needle revolutions. Rho signaling and associated actomyosin contractility was investigated with blebbistatin (100 μM) (Calbiochem, San Diego, CA) (Straight et al., 2003) and two different inhibitors of Rho kinase: Y-27632 (10 μM) (Biomol, Plymouth Meeting, PA), and H-1152 (10 μM) (Calbiochem). Rac signaling was inhibited with NCS23766 (117 μM) (Calbiochem). As a control, SP600125 (10 μM) (Calbiochem) was used a JNK-2 signaling inhibitor not involved in cytoskeletal remodeling. All inhibitors were solubilized directly in 37° HEPES PSS (similar results for SP600125 were obtained with and without DMSO). The addition of inhibitors was followed by a 10 min rest, then preload and needle rotation as above.

Histochemical staining, confocal microscopy, and morphometric analysis

Following the overnight rinse (described above), the needle was removed from the tissue and three subcutaneous tissue samples (each 10 × 10 mm) were dissected from the tissue flap. Each sample was placed flat on a glass slide. The sample that had included the needle was labeled "medial," and the other samples labeled "lateral right" and "lateral left," respectively (Fig. 1C). The slides were stained with Texas Red conjugated phalloidin (a specific stain for polymerized actin) and SYTOX nuclear stain, then imaged with a Bio-Rad MRC 1024 confocal microscope (Bio-Rad Microsciences, Hercules, CA), as previously described (Langevin et al., 2004). Each sample was divided longitudinally into three roughly equal-sized areas.

One field was imaged in the center of each area (nine fields per animal). Fields were chosen at low power by an individual blind to the study variable (preload or number of revolutions). Imaged fields were located in the center of each area without regard for needle position, since the needle track was not always visible. For each field, a stack of 20 (313×313 μm) images was acquired at a 1 μm inter-image interval. Image stacks were imported into the analysis software package MetaMorph (version 6.0; Universal Imaging Corporation, Downington, PA) for morphometric analysis. Cell body cross sectional area was measured as previously described (Langevin et al., 2005).

Statistical methods

Two-way analyses of variance (ANOVA) were used to test for differences in mean cell body cross sectional area in each experiment. In the first experiment, designed to examine the effect of varying preload, the two factors were preload [an across-subject factor with three levels [(0.2, 0.3, and 0.5 g)] and region [a within-subject factor with two levels (medial vs. lateral)]. For the second experiment designed to examine the effects of varying the number of needle revolutions, the two factors were number of revolutions [an across-subject factor with five levels [(0, 2, 4, 8, and 12)] and region [a within-subject factor with two levels (medial vs. lateral)]. Additional ANOVA's were performed to compare experimental conditions done at two needle revolutions in the presence of pharmacological inhibitors to those without inhibitors. In all experiments, data from lateral right and lateral left samples were combined into one lateral region. When the *F*-test from the ANOVA was significant ($P < 0.05$), Fisher's LSD was used to perform comparisons among means. Statistical analyses were performed using SAS statistical Software Version 8.02.

RESULTS

Effect of varying preload

Preload had a significant effect on cell body cross sectional area ($F_{2,8} = 12.3$, $P = 0.004$). Cross sectional area did not significantly change until a preload of 4.9 mN was applied to the tissue (Fig. 2). There was no evidence of significant differences in cell body cross sectional area between the regions of the tissue ($F_{1,8} = 3.4$, $P = 0.10$), nor was there evidence that the effect of preload was different across regions ($F_{2,8} = 0.4$, $P = 0.69$). Based on these results, we chose 2.9 mN as our preload in subsequent experiments investigating the effects of varying rotation.

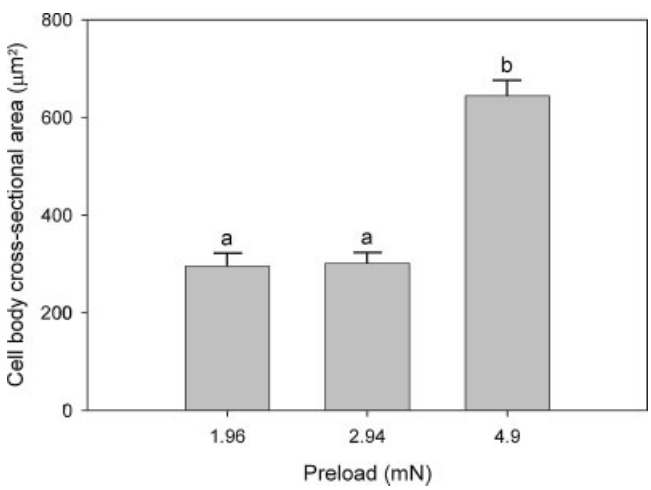

Fig. 2. Mean cell body cross sectional area with varying tissue preload. Values sharing a common letter are not significantly different. Error bars represent SE.

Effect of needle rotation

Two needle revolutions caused fibroblast cell bodies to become large and "sheet-like" with extensive spreading and lamellipodia formation (Fig. 3B,D). This was in contrast to the small cell bodies and long cytoplasmic processes seen with no rotation (Fig. 3A,C).

Statistical analysis of morphometric measurements showed that the number of needle revolutions had a significant effect on fibroblast cell body cross sectional area ($F_{4,28} = 6.9$, $P < 0.001$) (Fig. 4A, Table 1). Cell body cross sectional area peaked with two needle revolutions and decreased with further increases in rotation. The increase in mean cross sectional area from 0 to 2 needle revolutions was similar in magnitude to the difference produced by increasing the preload from 2.9 to 4.9 mN (Figs. 2 and 4).

With no rotation, fibroblast morphology was uniform throughout the tissue (Fig. $5A_2$–E_2). With rotation, the largest cells were seen in the medial samples (Fig. $5B_1$,D_1), with the exception of a 1 or 2 mm-wide band immediately adjacent to the needle where a "whorl" of connective tissue was often seen containing thin, elongated, spindle-shaped fibroblasts that were frequently distorted with processes that appeared broken and/or recoiled (Fig. 5, compare Fig $5C_1$,C_2). Morphometric examination of separate tissue regions revealed that the effect of rotation was somewhat more pronounced in the tissue samples closest to the needle (Fig. 4B, open bars), though there was no evidence that the rotation effect was region-specific ($F_{4,18} = 2.2$, $P = 0.10$).

Effect of pharmacological inhibitors

Based on the above results, pharmacological experiments were performed with two needle revolutions. Fibroblasts incubated with rotation in the presence of blebbistatin, Rho kinase inhibitors (Y-27632 and H-1152), and the Rac 1 inhibitor had small cell bodies (Fig. 6B–E). In contrast, fibroblasts incubated with rotation in the presence of the JNK-2 inhibitor had large cell bodies, similar in appearance to those incubated in the absence of inhibitors with needle rotation (Fig. 6F). Morphometric measurements showed that, when needle rotation was performed in the presence of blebbistatin, Rho kinase or Rac-1 inhibitors, mean cell body cross sectional area was significantly smaller compared with needle rotation without inhibitors (Fisher's LSD) (Fig. 7, Table 1). Thus, the increase in fibroblast cross-sectional area induced by acupuncture needle rotation was prevented by inhibition of actomyosin contractility as well as Rho and Rac signaling, but not JNK-2 signaling.

DISCUSSION

Acupuncture needle rotation caused fibroblast spreading and lamellipodia formation involving Rho and Rac signaling as well as actomyosin interaction. The results of this study therefore show that mechanical stimulation of subcutaneous tissue causes active fibroblast cytoskeletal remodeling involving mechanotransduction-based mechanisms. It is now well established that the cytoskeleton is an integrated and dynamic system within the cell that actively interacts with the extracellular matrix via specialized sites on the cell surface (actin-integrin focal adhesions) (Lauffenburger and Horwitz, 1996; Geiger and Bershadsky, 2001). Changes in cell shape (e.g., cell spreading during migration, neuronal growth cone extension, or cellular

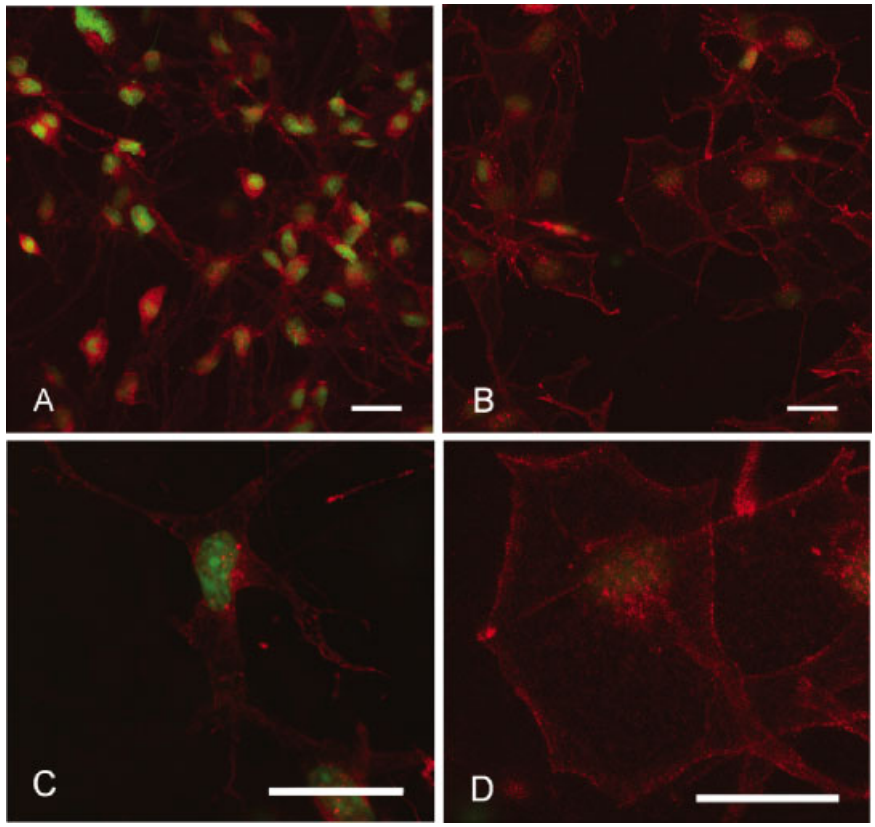

Fig. 3. **A**, **B**: Mouse subcutaneous tissue incubated for 30 min after acupuncture needle rotation (two revolutions) (B) compared with no rotation (A). **C**, **D**: Individual fibroblasts with rotation (D) and without rotation (C). All samples were stained with Texas-red conjugated phalloidin counter stained with SYTOX nucleic acid stain, and imaged with confocal microscopy. Scale bars, 40 μm. A and B are composite projections of stacks containing 20 optical sections taken at 1 μm intervals. C and D are projections of relevant optical sections containing the cells. [Color figure can be viewed in the online issue, which is available at www.interscience.wiley.com.]

response to mechanical substrate deformation) are accompanied by active and coordinated reorganizations of the cytoskeleton. These events include actin filament polymerization/depolymerization, microtubule assembly/disassembly, actomyosin contraction, and focal adhesion formation/disruption (Theriot and Mitchison, 1991; Ponti et al., 2004). Several Rho GTPase signaling molecules are known to play key roles in coordinating these processes (Rottner et al., 1999; Ridley, 2001). Rac induces the formation of focal adhesion complexes along the edge of lamellipodia, while Rho activates the transformation of these focal complexes into focal contacts via generation of myosin-II dependent tension (Geiger and Bershadsky, 2001). Recent evidence in addition suggests that Rho is involved in microtubule targeting, capture, and stabilization at focal adhesion sites (Ishizaki et al., 2001; Wittmann and Waterman-Storer, 2001) and that microtubules migrate toward focal adhesions in areas of externally applied tensile stress (Kaverina et al., 2002). Dynamic cytoskeletal mechanisms also are thought to play an important role in cell biomechanics by balancing internal tensile and compressive cellular forces with forces externally applied to the cell via the extracellular matrix (Wang et al., 2002; Ingber, 2003). According to this "cellular tensegrity" model, actomyosin contraction coupled to microfilaments generate cellular internal tension, while the microtubule network provides internal compressive forces (although some controversy exists as to whether microtubules are rigid-enough to fulfill this function) (Mitchison and Kirschner, 1984; Gittes et al., 1993; Mickey and Howard, 1995; Waterman-Storer and Salmon, 1997; Gupton et al., 2002; Stamenovic et al., 2002).

The active cellular responses found in this study are consistent with the above biochemical and biomechanical models of cytoskeletal function, and suggest the following sequence of events in response to acupuncture needle rotation: (1) winding and pulling of tissue from the periphery toward the needle; (2) initial pull of extracellular matrix on fibroblasts at existing focal contacts; (3) formation of lamellipodia (Rac-induced) in regions of the cell that are mechanically stimulated (predominantly in the plane of the pulled tissue); (4) increased actomyosin contraction (Rho-induced) without distinct stress fiber formation (due to the complex three-dimensional pattern of matrix attachments); (5) microtubule migration and stabilization; (6) increased intracellular tension, cell expansion, and flattening in the tissue plane until a new tension equilibrium is achieved between intracellular tension (actomyosin-driven) and two types of opposing forces: (a) extracellular matrix counter-tensional forces and (b) intracellular compressive forces provided by the expanded cytoskeleton. This proposed mechanism is illustrated in Figure 8. Such a mechanism, situated at the nexus of current biochemical and biomechanical understanding of mechanotransduction, would not only explain the cell shape changes observed in this study, but would also support the previously proposed concept that connective tissue

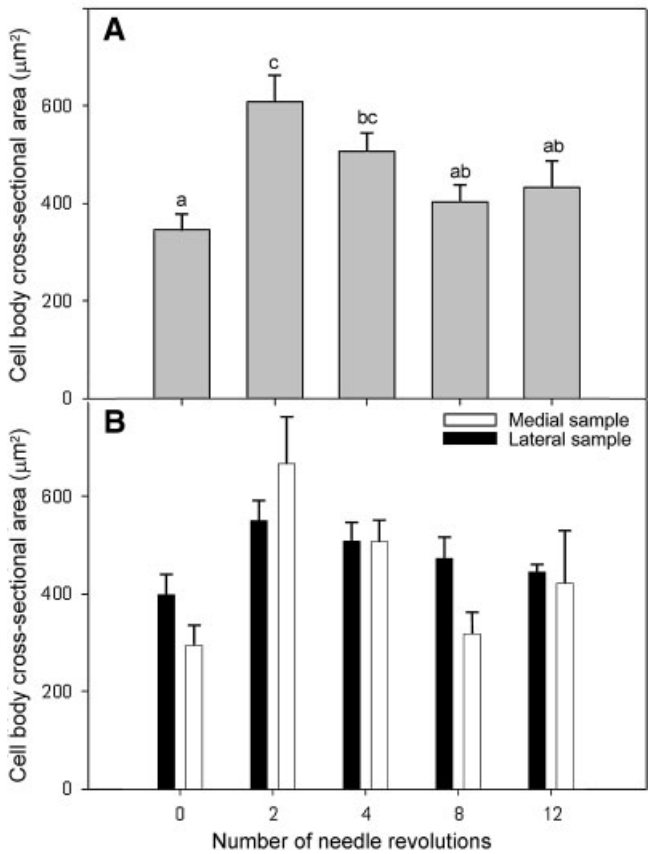

Fig. 4. Effect of increasing amounts of acupuncture needle rotation on mean fibroblast cell body cross sectional area. **A**: Overall effect of rotation in combined medial and lateral tissue samples. Values sharing a common letter are not statistically significant. **B**: Cell body cross-sectional area in medial (open bars) and lateral (solid bars) tissue samples. Error bars represent SE.

tension is actively regulated by fibroblasts (Eastwood et al., 1996).

An important effect of mechanotransduction is the regulation of mechanosensitive genes via signaling pathways linked to mechanically-induced cytoskeletal reorganization (Chiquet et al., 2003). Fibroblast cytoskeletal remodeling in response to acupuncture therefore may have effects on mechanotransduction-mediated gene expression and connective tissue matrix remodeling. Change in extracellular matrix composition days to weeks following acupuncture may cause modulation of sensory input from mechanosensory and nociceptor afferent neurons within connective tissue. As expected, acupuncture-induced changes in cell shape were not prevented by inhibition of JNK-2, which is consistent with its known functions (activation gene expression downstream of Rac and Cdc 42, and regulation of apoptosis (Coso et al., 1995; Minden et al., 1995)). Whether this type of mechanical stimulus causes JNK-2-mediated changes in gene expression will be an important topic for future studies.

We believe that an important aspect of this study is that it can serve to bridge the extensive knowledge on mechanotransduction derived from cell culture models to an eventual understanding of (1) the effect of mechanical forces on cells in vivo in both normal and diseased connective tissue, (2) how mechanical forces of a certain type, amplitude, and duration can be therapeutic, and (3) what "dose" of mechanical stimulation produces the optimal therapeutic effect. The fibroblast spreading induced by needle rotation was similar to that previously reported with stretching of subcutaneous tissue together with dermis (Langevin et al., 2005), showing that two different types of mechanical stimuli (tissue stretch and acupuncture) caused similar subcutaneous tissue fibroblast morphological responses. Thus, connective tissue mechanotransduction responses may be common to different types of therapeutic interventions using externally applied mechanical forces (e.g., physical therapy, massage, and acupuncture).

The importance of acupuncture needle manipulation techniques has been stressed in acupuncture texts since ancient times (Yang, 1991; Wu, 1993). These techniques typically consist of varying combinations of rotational and axial needle movements. The frequency, amplitude, and duration of these needle movements traditionally are believed key to optimize treatment outcome (O'Connor et al., 1981; Cheng, 1987). In this series of experiments, two revolutions of the acupuncture needle caused the greatest increase in fibroblast cell body cross sectional area. This amount of needle rotation caused cellular changes comparable to those of a surprisingly small amount of tissue load (1.96 mN (0.2 g)). This pattern of cellular response is reminiscent of biomechanical effects previously described in bone where smaller strain levels caused greater biological effects than larger ones (Brand and Stanford, 1994). Further studies will be important to examine cellular responses to smaller amounts of rotation between zero and two revolutions. The decreased spreading of fibroblasts with greater than two revolutions, on the other hand, may be due to cells sensing "too much" (or too rapid) external tension and letting go of existing adhesions, thus decreasing or delaying Rac-induced lamellipodia formation. Such a pattern (initial retraction followed cell respreading) was described in cultured cells in response to matrix traction (Petroll et al., 2004). It is also possible that the decreased cell spreading with increasing rotation was due to increased slippage at the

TABLE 1. Fibroblast corss sectional area measurements

Pharmacological inhibition	Drug	#Needle revolutions				
		0	2	4	8	12
None	None	348.4 ± 92.4 (8)	611.2 ± 141.0 (7)	510.3 ± 90.3 (6)	405.9 ± 93.1 (8)	435.5 ± 106.2 (4)
Actomyosin	Blebbistatin	—	392.1 ± 44.4 (3)	—	—	—
Rac 1	NSC23766	—	316.8 ± 118.9 (3)	—	—	—
Rho kinase	Y27632	—	346.8 ± 25.4 (3)	—	—	—
Rho kinase	H-1152	—	323.8 ± 86.2 (3)	—	—	—
JNK 2	Calbiochem 420119	—	492.9 ± 76.7 (3)	—	—	—

Results presented as mean ± SD fibroblast cross-sectional area in combined (media and lateral) tissue samples. Value in parentheses (N_{animal}); number of cells measured per animal ranged from 43 to 60 cells. Measurements are expressed in μm^2.

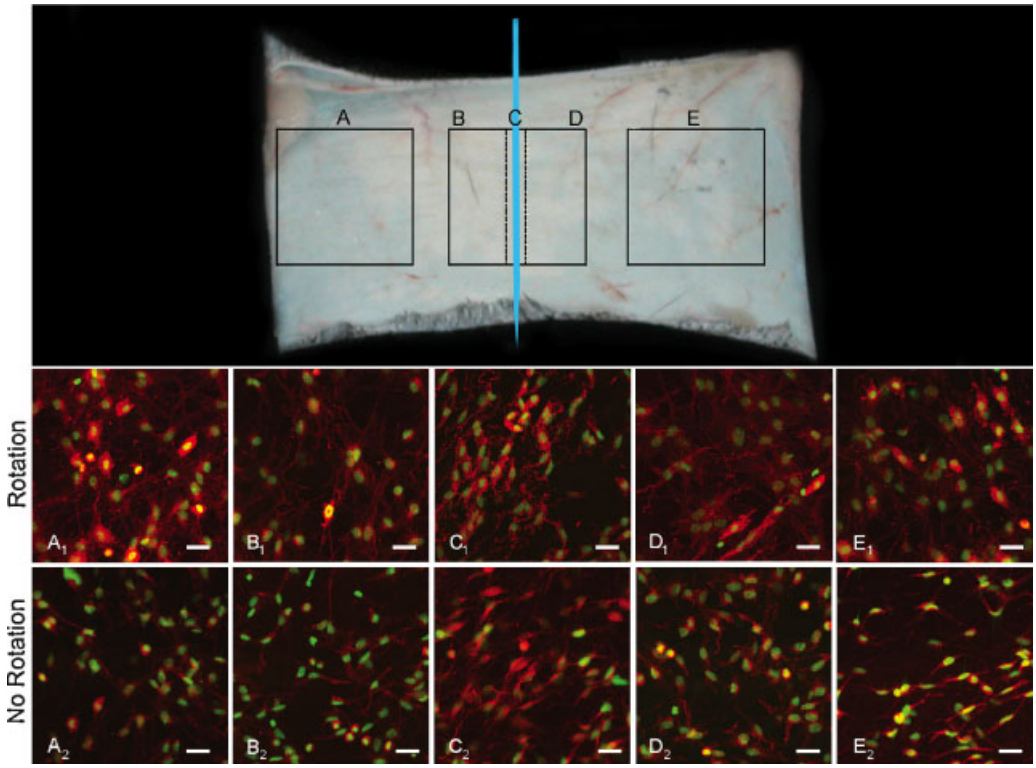

Fig. 5. Fibroblast morphology in different parts of the tissue with and without needle rotation (two revolutions). Tissue sample locations (**A–E**) are shown in top panel. With rotation, fibroblasts in tissue nearest the needle were spindle-shaped with processes that appeared undulating, twisted, or broken (C_1), while fibroblasts in the rest of the tissue were large and "sheet-like" (A_1, B_1, C_1, D_1). The largest cells with rotation were found within a zone 1–5 mm away from the needle (B_1,D_1). With no rotation, fibroblasts throughout the tissue had a similar "dendritic" appearance with small cell bodies and long branching processes (A_2–E_2). Scale bars, 40 μm. [Color figure can be viewed in the online issue, which is available at www.interscience.wiley.com.]

needle/tissue interface causing decreased tissue winding. We consider this unlikely based on the torque developing at the needle/tissue interface during rotation. Although the aim of this study was not to measure needle torque, we did collect indirect torque measurements by recording the amount of current passing through the motor during rotation. Mean (±SD) needle torque during four and eight needle revolutions were

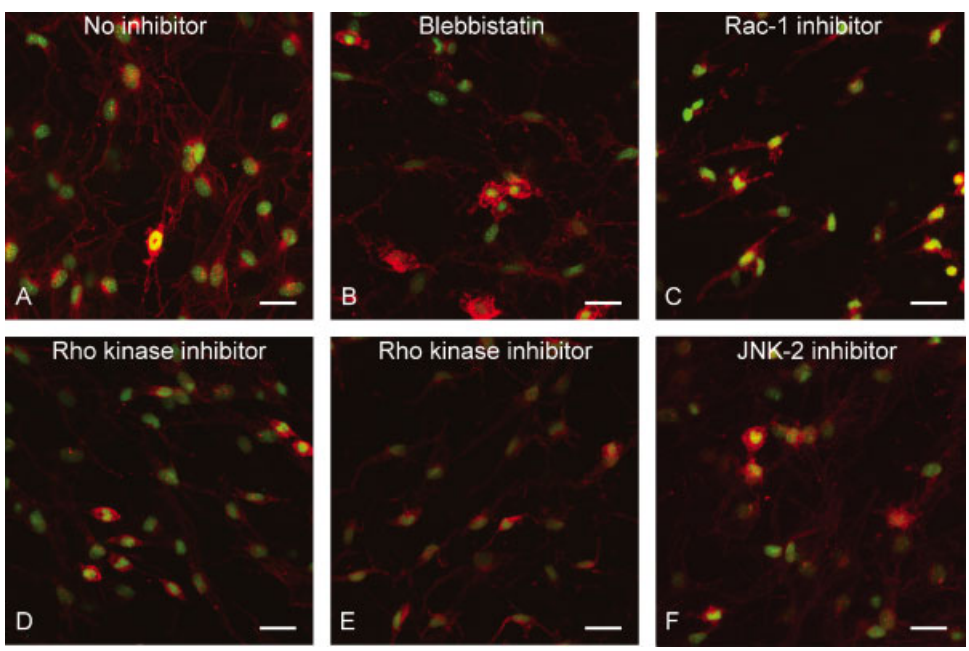

Fig. 6. Fibroblast morphology with needle rotation with and without pharmacological inhibitors. All samples received two needle revolutions. **A**: Control without inhibitor; (**B**) actomyosin contractility inhibitor (blebbistatin); (**C**) Rac-1 inhibitor (NCS23766); (**D**) Rho kinase inhibitor (Y27632), (**E**) Rho kinase inhibitor (H-1152); (**F**) JNK-2 inhibitor (SP600125). [Color figure can be viewed in the online issue, which is available at www.interscience.wiley.com.]

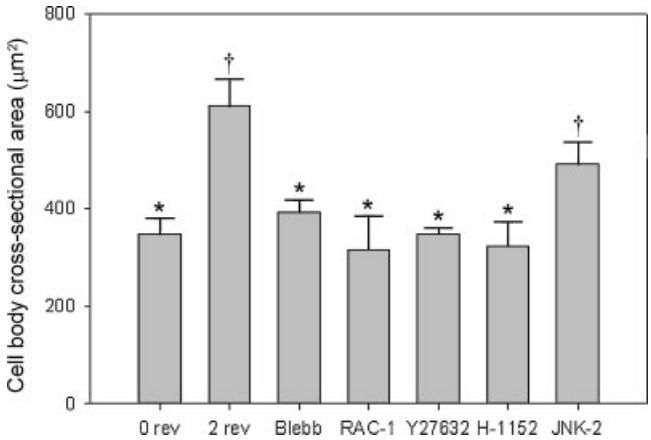

Fig. 7. Effect of pharmacological inhibitors on mean fibroblast cross sectional area, compared with 0 and 2 needle revolutions without inhibitors. All samples with inhibitors received two needle revolutions: Blebbistatin (actomyosin contractility inhibitor); Rac-1 inhibitor (NCS23766); Rho kinase inhibitor (Y27632), Rho kinase inhibitor (H-1152); JNK-2 inhibitor (SP600125). *indicates significant difference from two needle revolutions without inhibitor; †indicates significant difference from 0 needle revolutions without inhibitor. Error bars represent SE.

0.21 ± 0.14 and 0.77 ± 0.05 mNm, respectively. Torque during 2 needle revolutions was too low to be reliably detectable and 12 revolutions produced torques that were too large and saturated the motor current. This progressive increase in torque from 0 to 12 rotations therefore suggests that, in these experiments, the smaller cell cross sectional areas with increasing rotation was not due to the cells perceiving less mechanical force due to slippage. Although additional studies will be needed to determine whether a causal link exists between fibroblasts' response to mechanical stimulation and therapeutic effects (e.g., pain reduction), the dose-related physiological effects observed in this study may eventually prove to be important clinically.

Significant effects of rotation were present throughout the tissue, indicating the induction of an active response extending laterally over several centimeters. The largest cells were measured in the medial tissue samples corresponding to a 0.5 cm zone on both sides of the needle. Since the fibroblasts measured in the medial samples also included some of the thin spindle-shaped fibroblasts found in the immediate vicinity of the connective tissue "whorl" (Fig. $4C_1$), it is likely that mean cell cross sectional area in the medial tissue samples would have been even greater if these cells had been excluded. In order to mimic the clinical situation, the needle was not held in the final rotation position after the completion of rotation, but rather was allowed to remain free in the tissue during the dwell time. We did observe some amount of "spinning back" of the needle immediately after disconnection, but did not assess this quantitatively. The remaining whorl of connective tissue grossly observable after fixation suggests that the needle does not spin back completely, but that some amount of tissue winding remains present throughout the 30 min dwell time between needle rotation and tissue fixation.

A limitation of this study is that, since our imaging methods required tissue fixation, we could only assess cellular effects at one time point following needle rotation. We chose a 30 min dwell time between needle rotation and tissue fixation based on (1) a previous study of tissue stretch (Langevin et al., 2005) in which measurable effects of stretch occurred between 10 and 120 min after stretching the tissue and (2) because acupuncturists typically leave needles in place for 20–30 min after manipulation. Other possible effects of needle rotation that may occur between 0 and 30 min while the needle is still in place (e.g., increase in intracellular calcium or release of ATP) could be examined in future studies using live cell imaging techniques. Such effects may, for example, result in cell-to-cell signaling, which may contribute to spreading of the effect of acupuncture along connective tissue planes.

In acupuncture practice, the angle of needle insertion relative to the skin surface varies widely from very shallow (0–10°) to perpendicular (90°) depending on the clinical situation (Cheng, 1987). Because mouse subcutaneous tissue is very thin (50–100 μm), we chose to perform our quantitative experiments using a needle angle of 0° (needle parallel to the skin surface) in order to maximize the precision and consistency of needle placement within subcutaneous tissue and thus the reproducibility of our testing conditions. However, we obtained similar results using both parallel and perpendicular needle orientations (data not shown) suggesting that the basic phenomena observed in this study are present using a wide range of needling angles.

In summary acupuncture induced an active cytoskeletal response in connective tissue fibroblasts with extensive cell spreading and lamellipodia formation

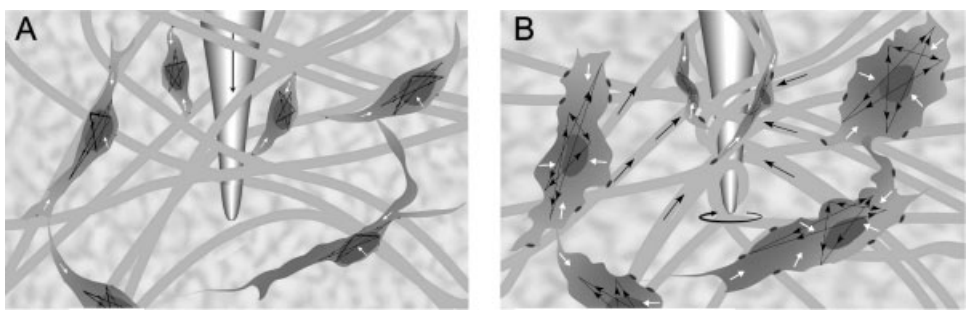

Fig. 8. Summary illustration representing proposed active fibroblast response to acupuncture needle rotation. Needle rotation (**B**) causes winding of collagen fibers around the needle and formation of a "whorl" of collagen and fibroblasts in the area immediately surrounding the needle. With small amounts of needle rotation, pulling of collagen fibers towards the needle causes fibroblasts further away from the needle to respond by changing shape, becoming large and "sheet-like" in marked contrasts with the small cell bodies and long branching processes ("dendritic" morphology) seen without needle rotation (**A**). After needle rotation, a new tension equilibrium is achieved between actomyosin-driven intracellular tension (intracellular white arrows) and two types of opposing forces: extracellular matrix counter-tensional forces (extracellular black arrows) and intracellular compressive forces provided by the expanded cytoskeleton (intracellular black arrows). Gray dots represent focal contacts.

involving Rho kinase, Rac signaling, and actomyosin contraction. This effect was measurable as an increase in fibroblast cross sectional area, which was greatest with two needle revolutions and decreased with further increases in rotation. A significant effect of rotation was present several centimeters away from the needle. This study constitutes an important step in understanding cellular mechanotransduction responses to externally applied mechanical forces in whole connective tissue. Further studies will address downstream effects of this cellular response (such as gene expression) leading to long term tissue changes that may translate into therapeutic mechanisms relevant to a wide range of treatments including physical therapy and massage as well as acupuncture.

ACKNOWLEDGMENTS

The authors thank Kirsten N. Storch and Alexander T. Danco for technical assistance, Debbie Stevens-Tuttle for help in preparing the manuscript, and Dr. Kenneth R. Cutroneo and Dr. Marilyn J. Cipolla for helpful discussions. This study was funded by the National Center for Complementary and Alternative Medicine Research Grant RO1-AT01121. Its contents are solely the responsibility of the authors and do not necessarily represent the official views of the National Center for Complementary and Alternative Medicine, National Institutes of Health.

LITERATURE CITED

Banes AJ, Tsuzaki M, Yamamoto J, Fischer T, Brigman B, Brown T, Miller L. 1995. Mechanoreception at the cellular level: The detection, interpretation, and diversity of responses to mechanical signals. Biochem Cell Biol 73(7–8):349–365.

Brand RA, Stanford CM. 1994. How connective tissues temporally process mechanical stimuli. Med Hypotheses 42(2):99–104.

Cheng X. 1987. Chinese acupuncture and moxibustion. In: Cheng X, editor. Chinese acupuncture and moxibustion, 1st edition. Beijing: Foreign Language Press. pp 322–329.

Chicurel ME, Chen CS, Ingber DE. 1998. Cellular control lies in the balance of forces. Curr Opin Cell Biol 10(2):232–239.

Chiquet M, Renedo AS, Huber F, Fluck M. 2003. How do fibroblasts translate mechanical signals into changes in extracellular matrix production? Matrix Biol 22(1):73–80.

Coso OA, Chiariello M, Yu JC, Teramoto H, Crespo P, Xu N, Miki T, Gutkind JS. 1995. The small GTP-binding proteins Rac1 and Cdc42 regulate the activity of the JNK/SAPK signaling pathway. Cell 81(7):1137–1146.

Eastwood M, Porter R, Khan U, McGrouther G, Brown R. 1996. Quantitative analysis of collagen gel contractile forces generated by dermal fibroblasts and the relationship to cell morphology. J Cell Physiol 166(1):33–42.

Geiger B, Bershadsky A. 2001. Assembly and mechanosensory function of focal contacts. Curr Opin Cell Biol 13(5):584–592.

Gittes F, Mickey B, Nettleton J, Howard J. 1993. Flexural rigidity of microtubules and actin filaments measured from thermal fluctuations in shape. J Cell Biol 120(4):923–934.

Grinnell F. 2003. Fibroblast biology in three-dimensional collagen matrices. Trends Cell Biol 13(5):264–269.

Gupton SL, Salmon WC, Waterman-Storer CM. 2002. Converging populations of f-actin promote breakage of associated microtubules to spatially regulate microtubule turnover in migrating cells. Curr Biol 12(22):1891–1899.

Hall A. 1998. Rho GTPases and the actin cytoskeleton. Science 279(5350):509–514.

Iatridis JC, Wu J, Yandow JA, Langevin HM. 2003. Subcutaneous tissue mechanical behavior is linear and viscoelastic under uniaxial tension. Connect Tissue Res 44(5):208–217.

Ingber DE. 2003. Tensegrity I. Cell structure and hierarchical systems biology. J Cell Sci 116(Pt 7):1157–1173.

Ishizaki T, Morishima Y, Okamoto M, Furuyashiki T, Kato T, Narumiya S. 2001. Coordination of microtubules and the actin cytoskeleton by the Rho effector mDia1. Nat Cell Biol 3(1):8–14.

Kaverina I, Krylyshkina O, Beningo K, Anderson K, Wang YL, Small JV. 2002. Tensile stress stimulates microtubule outgrowth in living cells. J Cell Sci 115(Pt 11):2283–2291.

Langevin HM, Churchill DL, Cipolla MJ. 2001a. Mechanical signaling through connective tissue: A mechanism for the therapeutic effect of acupuncture. FASEB J 15(12):2275–2282.

Langevin HM, Churchill DL, Fox JR, Badger GJ, Garra BS, Krag MH. 2001b. Biomechanical response to acupuncture needling in humans. J Appl Physiol 91(6):2471–2478.

Langevin HM, Churchill DL, Wu J, Badger GJ, Yandow JA, Fox JR, Krag MH. 2002. Evidence of connective tissue involvement in acupuncture. FASEB J 16(8):872–874.

Langevin HM, Cornbrooks CJ, Taatjes DJ. 2004. Fibroblasts form a body-wide cellular network. Histochem Cell Biol 122(1):7–15.

Langevin HM, Bouffard NA, Badger GJ, Iatridis JC, Howe AK. 2005. Dynamic fibroblast cytoskeletal response to subcutaneous tissue stretch ex vivo and in vivo. Am J Physiol Cell Physiol 288(3):C747–C756.

Lauffenburger DA, Horwitz AF. 1996. Cell migration: A physically integrated molecular process. Cell 84(3):359–369.

Mickey B, Howard J. 1995. Rigidity of microtubules is increased by stabilizing agents. J Cell Biol 130(4):909–917.

Minden A, Lin A, Claret FX, Abo A, Karin M. 1995. Selective activation of the JNK signaling cascade and c-Jun transcriptional activity by the small GTPases Rac and Cdc42Hs. Cell 81(7):1147–1157.

Mitchison T, Kirschner M. 1984. Microtubule assembly nucleated by isolated centrosomes. Nature 312(5991):232–237.

O'Connor J, Bensky D, yi xue yuan SZ. 1981. Acupuncture: A comprehensive text. Chicago: Eastland Press.

Petroll WM, Vishwanath M, Ma L. 2004. Corneal fibroblasts respond rapidly to changes in local mechanical stress. Invest Ophthalmol Vis Sci 45(10):3466–3474.

Ponti A, Machacek M, Gupton SL, Waterman-Storer CM, Danuser G. 2004. Two distinct actin networks drive the protrusion of migrating cells. Science 305(5691):1782–1786.

Ridley AJ. 2001. Rho family proteins: Coordinating cell responses. Trends Cell Biol 11(12):471–477.

Rottner K, Hall A, Small JV. 1999. Interplay between Rac and Rho in the control of substrate contact dynamics. Curr Biol 9(12):640–648.

Stamenovic D, Mijailovich SM, Tolic-Norrelykke IM, Chen J, Wang N. 2002. Cell prestress II. Contribution of microtubules. Am J Physiol Cell Physiol 282(3): C617–C624.

Straight AF, Cheung A, Limouze J, Chen I, Westwood NJ, Sellers JR, Mitchison TJ. 2003. Dissecting temporal and spatial control of cytokinesis with a myosin II Inhibitor. Science 299(5613):1743–1747.

Theriot JA, Mitchison TJ. 1991. Actin microfilament dynamics in locomoting cells. Nature 352(6331):126–131.

Wang N, Tolic-Norrelykke IM, Chen J, Mijailovich SM, Butler JP, Fredberg JJ, Stamenovic D. 2002. Cell prestress I. Stiffness and prestress are closely associated in adherent contractile cells. Am J Physiol Cell Physiol 282(3): C606–C616.

Waterman-Storer CM, Salmon ED. 1997. Actomyosin-based retrograde flow of microtubules in the lamella of migrating epithelial cells influences microtubule dynamic instability and turnover and is associated with microtubule breakage and treadmilling. J Cell Biol 139(2):417–434.

Wittmann T, Waterman-Storer CM. 2001. Cell motility: Can Rho GTPases and microtubules point the way? J Cell Sci 114(Pt 21):3795–3803.

Wu J-N. 1993. Ling shu, or, The spiritual pivot. Washington, D.C. Honolulu, Hawaii: Taoist Center; Distributed by University of Hawaii Press.

Yang J. 1991. The golden needle: And other odes of traditional acupuncture: Book two of Yang Jizhou's grand compendium (1601). Edinburgh, New York: Churchill Livingstone.